Two Time-Derivative Lorentz Material (2TDLM) Formulation of a Maxwellian Absorbing Layer Matched to a Lossy Medium

David C. Wittwer, *Member, IEEE,* and Richard W. Ziolkowski, *Fellow, IEEE*

***Abstract*—A two time-derivative Lorentz material (2TDLM) is introduced to define polarization and magnetization fields that lead to an absorbing layer that can be matched to a lossy dielectric medium. The 2TDLM is a generalization of the successful uniaxial polarization and magnetization time-derivative Lorentz material (TDLM) which has been introduced as an absorbing boundary condition for simulation regions dealing with lossless materials. Expressions are derived to describe the propagation of an arbitrary plane wave in this 2TDLM Maxwellian absorbing material. They are used to study the scattering from a semi-infinite 2TDLM half-space of an arbitrary plane wave incident upon it from a lossy isotropic dielectric medium. Matching conditions are derived which produce reflectionless transmission through such an interface for any angle of incidence and frequency. Numerical tests are given which demonstrate the effectiveness of the resulting 2TDLM absorbing layer.**

***Index Terms*—Lossy media, perfectly matched layers, time-domain analysis.**

I. Introduction

CONSIDERABLE effort has been expended in recent years both in the computational electromagnetics (CEM) [1]–[14] and applied mathematics communities [15], [16] toward the construction of highly efficient absorbing boundary conditions (ABC's) for reflectionless grid truncation of numerical simulators for Maxwell equations. Ideally, the perfect ABC would absorb electromagnetic energy incident from any angle with any polarization and at all frequencies. Reflectionless termination of simulation regions associated with, for instance, finite-difference time-domain (FDTD) and finite-element (FEM) methods require such ABC's. Currently, the most popular ABC is the perfect matched layer (PML) introduced by Berenger [1]. While this approach has achieved excellent numerical results, the requisite splitting of the field equations renders the PML non-Maxwellian. Moreover, recent stability analyses [15], [16] have shown the PML ABC to be weakly ill posed.

A variety of alternative approaches that are Maxwellian have appeared recently [7]–[14]. Most are based upon the uniaxial medium formulation given by Sachs *et al.* [7]. To effect the requisite matched material conditions, Ziolkowski [11]–[14], for example, engineers an uniaxial electric and magnetic medium by introducing time-derivative Lorentz material (TDLM) models for the polarization and magnetization fields and currents. The resulting TDLM ABC for matching to isotropic, homogeneous, lossless materials has been implemented in one-, two-, and three-dimensional [(1-D), (2-D), (3-D)] FDTD simulators and produces absorption levels comparable to the PML ABC. Steps toward physical realization of such Maxwellian absorbers with artificial electric and magnetic molecules have been proposed by Auzanneau and Ziolkowski [17]–[19].

Unfortunately, many practical simulation problems involving, for instance, microstrip transmission lines, microstrip patch antennas, and microwave/millimeter wave integrated circuits (MIC/MMIC), deal with lossy substrates. Accurate simulations of these problems necessitate termination of the simulation region with an ABC matched to these lossy dielectrics. Berenger's PML ABC cannot be applied in this case. The development of a potentially physically realizable material that can lead to a generalization of the TDLM ABC to simulation regions dealing with general lossy dielectrics is the focus of this paper.

Beginning in Section II, the scattering of an obliquely incident plane wave from the interface between a lossy dielectric medium and a general biaxial anisotropic medium is described. The properties of the biaxial medium that are required for it to function as an ideal reflectionless medium are identified. In Section III, a physical material model is introduced, the two time-derivative Lorentz material (2TDLM) model, which allows this biaxial medium to become an ideal electromagnetic absorber. In Section IV, the governing differential equations describing a 2TDLM layer are coupled with Maxwell's equations into a state-space form for implementation in a numerical FDTD simulator. The explicit discretized forms of this 2TDLM layer system are provided in [20]. Several validation cases in one, two, and three dimensions have been completed; these results are summarized in Section IV. They demonstrate the effective absorption properties of the 2TDLM layer.

There have been a number of recent extensions of the PML ABC to lossy media and evanescent wave applications that are relevant to our absorber studies. Gedney in [21] and in [22, ch.

Manuscript received February 27, 1998; revised March 5, 1999. The work by D. C. Wittwer was supported in part by the Radar Design Center, Raytheon Systems Company, Tucson, AZ, through the Doctoral Fellowship Program. The work by R. W. Ziolkowski was supported in part by the Office of Naval Research under Grant N0014-95-1-0636 and by the Air Force Office of Scientific Research, Air Force Material Command, USAF, under Grant F49620-96-1-0039. The views and conclusions contained herein are those of the author and should not be interpreted as necessarily representing the Office of Naval Research or the Air Force Office of Scientific Research or the U.S. Government.

The authors are with the Electromagnetics Laboratory, Department of Electrical and Computer Engineering, University of Arizona, Tucson, AZ 85721-0104 USA.

Publisher Item Identifier S 0018-926X(00)01662-8.

5] develops an uniaxial PML (UPML) ABC that avoids the field splitting associated with the Berenger PML ABC. Results for the UPML ABC applied to a simple 2-D lossy medium test case are given. Lau *et al.* [23], Fang and Wu [24], and Liu [25] introduce variations of the Berenger PML ABC to deal with evanescent wave and lossy media problems. These approaches use the stretched coordinate ideas and normal field splitting associated with the Berenger PML ABC. Additional 2-D lossy media examples were discussed. Rappaport and Winton [26] have demonstrated the need for lossy media ABC's with their modeling of ground probing radar signals in lossy dispersive soil. Further issues associated with ABC's for various media situations are reviewed in [22]. The actual development of a complete 3-D ABC for lossy media based upon the 2TDLM model and its numerical implementation have been left to a companion paper [20]. We concentrate here on the material aspects of the 2TDLM model and its potential for the development of a useful absorbing slab. Consequently, we do not deal with any evanescent wave issues.

II. Plane Wave Scattering From an Interface Between a Biaxial Medium and an Isotropic Lossy Electric and Magnetic Medium

Consider a plane wave propagating in an isotropic lossy electric (relative permittivity ϵ_r and electric conductivity σ) and magnetic (relative permeability μ_r and magnetic conductivity σ^*) medium (Region I) that is obliquely incident upon a semi-infinite anisotropic medium (Region II), as illustrated in Fig. 1. The general obliquely-incident 3-D plane wave can be reduced to two orthogonal TE and TM plane wave problems [27]. Let $\vec{k}$ lie in the xz-plane with the normal to the interface in the $\hat{z}$ direction. We have followed the analysis presented originally in [7] but retaining all constitutive terms (i.e., ϵ_r, μ_r, σ, σ^* are carried throughout the entire calculation). We have carried all of these terms to a point in our argument which does not restrict its generality. However, since we are interested in the special case of lossy dielectrics (i.e., lossy, nonmagnetic materials), we shall restrict our explicit display of the results to that case.

An isotropic lossy medium in Region I is defined by setting $[\epsilon]/\epsilon_0 = \hat{\epsilon}_r[I]$ and $[\mu]/\epsilon_0 = \hat{\mu}_r[I]$ where $[I]$ is the unit tensor and the lossy relative permittivity and permeability are given by complex scalar expressions containing the electric and magnetic loss terms, viz:

$$\hat{\epsilon}_r = (\epsilon_r - j\sigma/\omega\epsilon_0), \qquad \hat{\mu}_r = (\mu_r - j\sigma^*/\omega\mu_r). \quad (1)$$

In Region II, we assume the anisotropic medium is biaxial in the same manner as was done in [11] for matching a layer to a lossless medium. A biaxial electric and magnetic medium may be represented in the most general sense by permittivity and permeability tensors of the form

$$\frac{[\epsilon]}{\epsilon_0} = \begin{pmatrix} a_e & 0 & 0 \\ 0 & b_e & 0 \\ 0 & 0 & c_e \end{pmatrix} \qquad \frac{[\mu]}{\mu_0} = \begin{pmatrix} a_m & 0 & 0 \\ 0 & b_m & 0 \\ 0 & 0 & c_m \end{pmatrix} \quad (2)$$

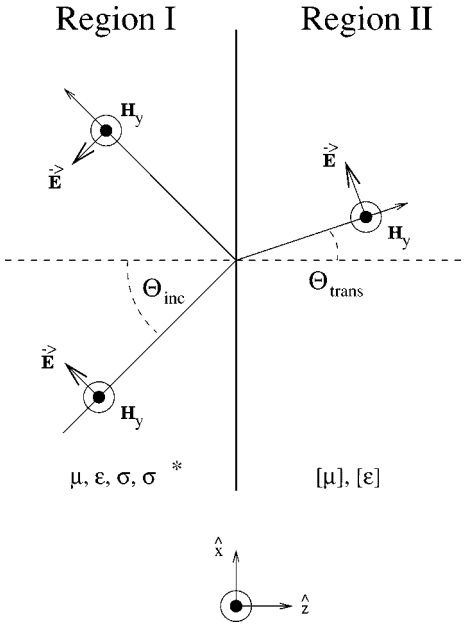

Fig. 1. Interface definition: parallel polarization.

where we have further introduced the complex coefficients

$$\hat{a}_e = \left(a_e - j\frac{\sigma}{\omega\epsilon_0}\right), \quad \hat{b}_m = \left(b_m - j\frac{\sigma^*}{\omega\mu_0}\right), \quad \hat{c}_e = \left(c_e - j\frac{\sigma}{\omega\epsilon_0}\right) \quad (3)$$

associated with the TM polarization and the complex coefficients

$$\hat{a}_m = \left(a_m - j\frac{\sigma^*}{\omega\mu_0}\right), \quad \hat{b}_e = \left(b_e - j\frac{\sigma}{\omega\epsilon_0}\right), \quad \hat{c}_m = \left(c_m - j\frac{\sigma^*}{\omega\mu_0}\right) \quad (4)$$

associated with the TE polarization. This is analogous to the usual method of generalizing lossless problems to their lossy counterparts.

Plane waves and the corresponding dispersion relations, wave impedances, and wave numbers are constructed in a straightforward manner. Then, introducing a plane wave incident from Region I onto Region II, one can obtain the reflection and transmission coefficients associated with the interface between Regions I and II for each polarization. It is readily shown that we have two independent variables, i.e., two degrees of freedom, $\hat{b}_e$ and $\hat{b}_m$, to satisfy the systems for the cases of a TE or a TM polarized incident plane wave. The conditions to affect a reflectionless scattering for each polarization are readily derived. For instance, one finds in the TE case that the coefficients of the permittivity and permeability tensors must satisfy the relations: $\hat{a}_e = (\hat{\epsilon}_r/\hat{\mu}_r)\hat{b}_m$ and $\hat{c}_e = (\hat{\epsilon}_r\hat{\mu}_r)/\hat{b}_m$. The complementary procedure is carried out in the same manner for the TM case. One finds that in order to realize reflectionless scattering for an arbitrarily polarized plane wave, i.e., simultaneously for both the TE and TM polarized components of the incident plane wave, that the electric and magnetic material coefficients must satisfy $\hat{b}_e = \hat{\epsilon}_r\hat{b}_m/\hat{\mu}_r$. This relation is equivalent to requiring that both transverse wave numbers must be continuous across the Region

I–II interface. Summarizing these results, this means the permittivity and permeability tensors must have the forms

$$\frac{[\epsilon]}{\epsilon_0} = \begin{pmatrix} [\hat{\epsilon}_r/\hat{\mu}_r]\hat{b}_m & 0 & 0 \\ 0 & [\hat{\epsilon}_r/\hat{\mu}_r]\hat{b}_m & 0 \\ 0 & 0 & \hat{\epsilon}_r\hat{\mu}_r/\hat{b}_m \end{pmatrix}$$
$$\frac{[\mu]}{\mu_0} = \begin{pmatrix} \hat{b}_m & 0 & 0 \\ 0 & \hat{b}_m & 0 \\ 0 & 0 & \hat{\mu}_r^2/\hat{b}_m \end{pmatrix}. \tag{5}$$

Note that the continuity of the transverse wavenumbers at the interface necessarily excludes equality of the normal wavenumbers. This results in different propagation velocities into the material for each polarization. Considering that our Region II material will be designed as an absorber, this will not cause a problem as one polarization will be simply damped faster than the other.

It is important to notice that these tensors will only be dual for the lossless free-space case where $\epsilon_r = 1$ and $\mu_r = 1$. For this case, the expressions derived in [7] are recovered.

III. Two Time-Derivative Lorentz Material Model

As found in [11], a susceptibility model that provides broad bandwidth absorption characteristics can be developed if the polarization (magnetization) of the medium is driven with contributions from time derivatives of the electric (magnetic) fields. Electric and magnetic field time derivative contributions to the polarization and magnetization fields can occur in a linear medium when it has both electric and magnetic properties. This means we can rewrite $[\epsilon]$ and $[\mu]$ in the form of complex susceptibilities χ. All that is required is that we find a suitable model for χ to specify completely the properties of the medium.

In order to simplify the analysis we will restrict the materials to which we will match the absorber. We now consider only nonmagnetic materials having $\hat{\mu}_r$ equal to unity and $\sigma^* = 0$. It is important to keep in mind that this restriction is not a requirement but merely a simplification of the analysis to problems most often encountered in engineering applications. Making this specialization reduces the complex coefficients in Region I to the form $\hat{\epsilon}_r = (\epsilon_r - j\sigma/\omega\epsilon_0)$, $\hat{\mu}_r = 1$. We now make the choice $\hat{b}_m = 1 + \chi^m$.

The tensors resulting from (5) are then

$$[\chi^e] = \frac{[\epsilon]}{\epsilon_0} - [1] = \begin{bmatrix} \chi^e_{xx} & 0 & 0 \\ 0 & \chi^e_{yy} & 0 \\ 0 & 0 & \chi^e_{zz} \end{bmatrix}$$
$$= \begin{pmatrix} \hat{\epsilon}_r(1+\chi^m)-1 & 0 & 0 \\ 0 & \hat{\epsilon}_r(1+\chi^m)-1 & 0 \\ 0 & 0 & \dfrac{\hat{\epsilon}_r}{(1+\chi^m)} - 1 \end{pmatrix} \tag{6}$$

$$[\chi^m] = \frac{[\mu]}{\mu_0} - [1] = \begin{bmatrix} \chi^m_{xx} & 0 & 0 \\ 0 & \chi^m_{yy} & 0 \\ 0 & 0 & \chi^m_{zz} \end{bmatrix}$$
$$= \begin{pmatrix} \chi^m & 0 & 0 \\ 0 & \chi^m & 0 \\ 0 & 0 & \dfrac{1}{(1+\chi^m)} - 1 \end{pmatrix}. \tag{7}$$

As was done in [11]–[14], one can introduce a generalization of the Lorentz model for the polarization and magnetization fields that includes time derivatives of the driving fields as source terms. For instance, the $\hat{x}$-directed polarization and magnetization fields in such a material would be assumed to satisfy a linear two time-derivative Lorentz material (2TD-LM) model, hence, have the forms

$$\frac{\partial^2}{\partial t^2}\mathcal{P}_x + \Gamma\frac{\partial}{\partial t}\mathcal{P}_x + \omega_o^2\mathcal{P}_x = \epsilon_o\left(\omega_p^2\chi^e_\alpha\mathcal{E}_x + \omega_p\chi^e_\beta\frac{\partial}{\partial t}\mathcal{E}_x + \chi^e_\gamma\frac{\partial^2}{\partial t^2}\mathcal{E}_x\right) \tag{8}$$

$$\frac{\partial^2}{\partial t^2}\mathcal{M}_x + \Gamma\frac{\partial}{\partial t}\mathcal{M}_x + \omega_o^2\mathcal{M}_x = \omega_p^2\chi^m_\alpha\mathcal{H}_x + \omega_p\chi^m_\beta\frac{\partial}{\partial t}\mathcal{H}_x + \chi^m_\gamma\frac{\partial^2}{\partial t^2}\mathcal{H}_x \tag{9}$$

where ω_0 is the resonance frequency and $\Gamma^{e,m}$ is the width of that resonance. Note the introduction of the second-time derivative; this is different from the formulation in [11]–[14]. The second-time derivative is required here to account for the loss in the medium. The terms $\chi^{e,m}_\alpha$, $\chi^{e,m}_\beta$, and $\chi^{e,m}_\gamma$ represent, respectively, the coupling of the electric (magnetic) field and its first- and second-time derivatives to the local charge motion. The term ω_p can be viewed as the plasma frequency associated with those charges. This 2TDLM model leads, for example, to the following frequency-domain electric and magnetic susceptibilities

$$\chi^e_{xx}(\omega) = \frac{P_x}{\epsilon_0 E_x} = \frac{\omega_p^2\chi^e_\alpha + j\omega\omega_p\chi^e_\beta - \omega^2\chi^e_\gamma}{-\omega^2 + j\omega\Gamma^e + \omega_0^2} \tag{10}$$

$$\chi^m_{xx}(\omega) = \frac{M_x}{H_x} = \frac{\omega_p^2\chi^m_\alpha + j\omega\omega_p\chi^m_\beta - \omega^2\chi^m_\gamma}{-\omega^2 + j\omega\Gamma^m + \omega_0^2}. \tag{11}$$

Ziolkowski [11] presents a proof that defines when a broad band absorber is realized. The desired conditions are obtained if the anisotropic 2TDLM medium is designed such that $\chi^{e,m}_\alpha$, $\chi^{e,m}_\beta$, $\chi^{e,m}_\gamma \geq 0$, and $\omega \gg \omega_0$, $\omega_p \gg \Gamma^{e,m}$. This choice gives the desired form of the 2TDLM susceptibilities. In particular, the transverse components of the magnetic susceptibility can be assigned to have the form

$$\chi^m_{xx,\,yy}(\omega) = \frac{M_{x,\,y}}{H_{x,\,y}} = \chi^m = -\frac{\omega_p^2}{\omega^2}\chi^m_\alpha - j\frac{\omega_p\chi^m_\beta}{\omega} + \chi^m_\gamma. \tag{12}$$

The values for χ^m_α, χ^m_β, and χ^m_γ may be determined by forcing continuity of the material properties and, hence, the impedance across the interface. From (5) we know that the permeability is directly related to $\hat{b}_m$. Clearly then, we need to set $\chi^m_\alpha = \chi^m_\beta = \chi^m_\gamma = 0$ at the interface between Regions I and II. On the other hand, from (12) we recognize that the χ^m_α and χ^m_γ terms are responsible, respectively, for a static (dc) contribution and a frequency dependent contribution in the real part of the permeability, while the χ^m_β term is responsible for a frequency dependent loss. Since we desire the loss to increase as the wave propagates into the absorber (Region II), we then choose to set

$$\chi^m_\alpha = 0 \tag{13}$$

$$\chi^m_\beta = \frac{\sigma}{\omega_p^2\,\epsilon_0}\,\overline{\zeta}(z) \tag{14}$$

$$\chi^m_\gamma = 0 \tag{15}$$

where $\overline{\zeta}(z)$ is a profile function whose value is zero at the interface and whose maximum value $\overline{\zeta}_{\max}$ will be fixed by the simulation problem. The explicit loss tangent coefficient $\tan\delta = \sigma/(\omega_p\epsilon_0)$ is included here for notational and magnitude convenience; in particular, it shows that the term $\omega_p\chi_\beta^m$ can be normalized to a more manageable value.

Consequently, the corresponding transverse components of the magnetic susceptibilities then have the form

$$\chi_{xx,\,yy}^m(\omega) = \frac{M_{x,\,y}}{H_{x,\,y}} = \frac{j\,\omega\,\omega_p\chi_\beta^m}{-\omega^2} = -j\frac{\omega_p\chi_\beta^m}{\omega} \tag{16}$$

and, similarly, the longitudinal component of the magnetic susceptibility has the form

$$\chi_{zz}^m(\omega) = \frac{M_z}{H_z} = \frac{1}{1 - j\omega\omega_p\chi_\beta^m/\omega^2} - 1. \tag{17}$$

Therefore, the frequency-domain expressions for the magnetization fields are

$$-\omega^2 M_{x,\,y} = j\omega\omega_p\chi_\beta^m H_{x,\,y} \tag{18}$$

$$-\omega^2 M_z + j\omega\omega_p\chi_\beta^m M_z = -\,j\omega\omega_p\chi_\beta^m H_z. \tag{19}$$

To find the corresponding expressions for the polarization fields, reconsider now the impedance ratio $\hat{\mu}_r/\hat{\epsilon}_r$ in Region I. Because of the choice that was made for $\hat{b}_m$, we find that this ratio remains the same in Region II if it has the following form:

$$\frac{\mu_r}{\left(\epsilon_r - j\dfrac{\sigma}{\omega\epsilon_0}\right)} = \frac{\mu_r}{\left(\epsilon_r - j\dfrac{\sigma}{\omega\epsilon_0}\right)}\frac{\left(1 - j\dfrac{\omega_p\chi_\beta^m}{\omega}\right)}{\left(1 - j\dfrac{\omega_p\chi_\beta^m}{\omega}\right)}. \tag{20}$$

This choice guarantees that the impedance in Region II will always be matched to its value in Region I. Due to the form of the denominator of this expression, we recognize that $\chi_{xx,\,yy}^e$ must then also have a 2TDLM form. The transverse components of the electric susceptibility are of the form

$$\begin{aligned}\chi_{xx,\,yy}^e(\omega) &= \frac{P_{x,\,y}}{\epsilon_0 E_{x,\,y}} \\ &= \hat{\epsilon}_r[1 + \chi^m(\omega)] - 1 \\ &= -\frac{\sigma}{\omega^2\epsilon_0}\omega_p\chi_\beta^m - j\left(\frac{\sigma}{\omega\epsilon_0} + \epsilon_r\frac{\omega_p\chi_\beta^m}{\omega}\right) \\ &\quad + (\epsilon_r - 1).\end{aligned} \tag{21}$$

This expression is matched to the 2TDLM model for the electric susceptibility, i.e., $\chi_{xx,\,yy}^e(\omega) \approx -(\omega_p/\omega)^2\chi_\alpha^e - j(\omega_p\chi_\beta^e)/\omega + \chi_\gamma^e$, if we identify the coefficients

$$\chi_\alpha^e = \left(\frac{\sigma}{\omega_p\epsilon_0}\right)\chi_\beta^m \tag{22}$$

$$\chi_\beta^e = \frac{\sigma}{\omega_p\epsilon_0} + \epsilon_r\chi_\beta^m \tag{23}$$

$$\chi_\gamma^e = \epsilon_r - 1. \tag{24}$$

The longitudinal component of the electric susceptibility tensor is then fixed to be

$$\begin{aligned}\chi_{zz}^e(\omega) &= \frac{P_z}{\epsilon_0 E_z} \\ &= \frac{\hat{\epsilon}_r}{[1 + \chi^m(\omega)]} - 1 \\ &= \frac{-\omega^2(\epsilon_r - 1) + j\omega\left(\dfrac{\sigma}{\epsilon_0} - \omega_p\chi_\beta^m\right)}{-\omega^2 + j\omega\omega_p\chi_\beta^m}.\end{aligned} \tag{25}$$

The polarization fields may then be represented in the frequency domain by

$$\begin{aligned}&-\omega^2 P_{x,\,y} \\ &\quad = \epsilon_0\omega_p^2\chi_\alpha^e E_{x,\,y} + j\omega\epsilon_0\omega_p\chi_\beta^e E_{x,\,y} - \omega^2\epsilon_0\chi_\gamma^e E_{x,\,y}\end{aligned} \tag{26}$$

$$\begin{aligned}&-\omega^2 P_z + j\omega\omega_p\chi_\beta^m P_z \\ &\quad = -\omega^2\epsilon_0(\epsilon_r - 1)E_z + j\omega\epsilon_0\left(\frac{\sigma}{\epsilon_0} - \omega_p\chi_\beta^m\right)E_z.\end{aligned} \tag{27}$$

With all of the susceptibility terms now well defined, it remains to develop a consistent set of ordinary differential equations that may be easily implemented in a FDTD code. In the general sense, Maxwell's equations including the polarization and magnetization fields are

$$-\nabla\times\vec{\mathcal{E}} = \frac{\partial}{\partial t}[\mu]\vec{\mathcal{H}} + \frac{\partial}{\partial t}\vec{\mathcal{M}} \tag{28}$$

$$\nabla\times\vec{\mathcal{H}} = \frac{\partial}{\partial t}[\epsilon]\vec{\mathcal{E}} + \frac{\partial}{\partial t}\vec{\mathcal{P}}. \tag{29}$$

The time-domain differential equations for the polarization and magnetization fields may be recovered by identifying multiplication by $j\omega$ in the frequency domain as equivalent to differentiation with respect to time in the temporal domain. Thus, the time-domain expression for the polarization and magnetization fields are found, respectively, from (18), (19), (26), and (27)

$$\frac{\partial^2}{\partial t^2}\mathcal{M}_{x,\,y} = \omega_p\chi_\beta^m\frac{\partial}{\partial t}\mathcal{H}_{x,\,y} \tag{30}$$

$$\frac{\partial^2}{\partial t^2}\mathcal{M}_z + \omega_p\chi_\beta^m\frac{\partial}{\partial t}\mathcal{M}_z = -\,\omega_p\chi_\beta^m\frac{\partial}{\partial t}\mathcal{H}_z \tag{31}$$

$$\frac{\partial^2}{\partial t^2}\mathcal{P}_{x,\,y} = \epsilon_0\omega_p^2\chi_\alpha^e\mathcal{E}_{x,\,y} + \epsilon_0\omega_p\chi_\beta^e\frac{\partial}{\partial t}\mathcal{E}_{x,\,y} + \epsilon_0\chi_\gamma^e\frac{\partial^2}{\partial t^2}\mathcal{E}_{x,\,y} \tag{32}$$

$$\begin{aligned}&\frac{\partial^2}{\partial t^2}\mathcal{P}_z + \omega_p\chi_\beta^m\frac{\partial}{\partial t}\mathcal{P}_z \\ &\quad = \epsilon_0\chi_\gamma^e\frac{\partial^2}{\partial t^2}\mathcal{E}_z + \epsilon_0\left(\frac{\sigma}{\epsilon_0} - \omega_p\chi_\beta^m\right)\frac{\partial}{\partial t}\mathcal{E}_z.\end{aligned} \tag{33}$$

We introduce the polarization and magnetizations currents

$$\mathcal{K}_{x,\,y} = \frac{\partial}{\partial t}\mathcal{M}_{x,\,y} - \omega_p\chi_\beta^m\mathcal{H}_{x,\,y} \tag{34}$$

$$\mathcal{K}_z = \frac{\partial}{\partial t}\mathcal{M}_z \tag{35}$$

$$\mathcal{J}_{x,\,y} = \frac{\partial}{\partial t}\mathcal{P}_{x,\,y} - \epsilon_0\omega_p\chi_\beta^e\mathcal{E}_{x,\,y} - \epsilon_0\chi_\gamma^e\frac{\partial}{\partial t}\mathcal{E}_{x,\,y} \tag{36}$$

$$\mathcal{J}_z = \frac{\partial}{\partial t}\mathcal{P}_z - \epsilon_0\chi_\gamma^e\frac{\partial}{\partial t}\mathcal{E}_z - \sigma\mathcal{E}_z \tag{37}$$

so that we may now treat a self-consistent set of first-order equations in state–space form. Substitution of the expressions for the

currents into (28), (29), and (30)–(33) yields the desired equation set

$$\frac{\partial}{\partial t}\mathcal{E}_{x,y}+\frac{\omega_p\chi^e_\beta}{1+\chi^e_\gamma}\mathcal{E}_{x,y} = \frac{1}{\epsilon_0\left(1+\chi^e_\gamma\right)}\left(\nabla\times\vec{\mathcal{H}}\right)_{x,y}-\frac{1}{\epsilon_0\left(1+\chi^e_\gamma\right)}\mathcal{J}_{x,y} \tag{38}$$

$$\frac{\partial}{\partial t}\mathcal{E}_{z}+\frac{\sigma}{\epsilon_0\left(1+\chi^e_\gamma\right)}\mathcal{E}_{z} = \frac{1}{\epsilon_0\left(1+\chi^e_\gamma\right)}\left(\nabla\times\vec{\mathcal{H}}\right)_{z}-\frac{1}{\epsilon_0\left(1+\chi^e_\gamma\right)}\mathcal{J}_{z} \tag{39}$$

$$\frac{\partial}{\partial t}\mathcal{J}_{x,y}=\epsilon_o\omega_p^2\chi^e_\alpha\mathcal{E}_{x,y} \tag{40}$$

$$\frac{\partial}{\partial t}\mathcal{J}_{z}+\omega_p\chi^m_\beta\mathcal{J}_z = -\left[\epsilon_0\omega_p\chi^m_\beta\left(1+\chi^e_\gamma\right)\right]\frac{\partial}{\partial t}\mathcal{E}_z-\sigma\omega_p\chi^m_\beta\mathcal{E}_z \tag{41}$$

$$\frac{\partial}{\partial t}\mathcal{H}_{x,y}+\omega_p\chi^m_\beta\mathcal{H}_{x,y}=-\frac{1}{\mu_0}\left(\nabla\times\vec{\mathcal{E}}\right)_{x,y} \tag{42}$$

$$\frac{\partial}{\partial t}\mathcal{H}_{z}=-\frac{1}{\mu_0}\left(\nabla\times\vec{\mathcal{E}}\right)_{z}-\mathcal{K}_z \tag{43}$$

$$\frac{\partial}{\partial t}\mathcal{K}_{z}+\omega_p\chi^m_\beta\mathcal{K}_z=-\omega_p\chi^m_\beta\frac{\partial}{\partial t}\mathcal{H}_z. \tag{44}$$

We note that none of the polarization or magnetization field components need to be included in this set. This greatly simplifies the computational aspects of implementing a 2TDLM absorbing layer.

IV. Numerical Implementation and Validation Results

It is now left to implement the 2TDLM model into a FDTD simulator. The loss in the 2TDLM slab is gradually introduced through the term $\omega_p\,\chi^m_\beta$. To correlate with the results in [20], we set

$$\omega_p\,\chi^m_\beta=\zeta(z)=\zeta_{\max}\left[(z-z_{\min})/(z_{\max}-z_{\min})\right]^m \tag{45}$$

where $\zeta_{\max}=\overline{\zeta}_{\max}\tan\delta$. The function $\zeta(z)$ is the profile function associated with the slab. Setting $m=2$ causes the loss to have a quadratic profile in the slab. The slab is defined by $z_{\min}$ and $z_{\max}$ and is the only region where the 2TDLM is implemented. The time derivative of the electric (magnetic) field on the right-hand side of (41) [(44)] is replaced by the expression in (39) [(43)]. This substitution along with the explicit material relations (13)–(15) and (22)–(24) leads from (38)–(44) to the following set of differential equations that may be implemented with a second-order differencing scheme and that preserves the leap frog paradigm

$$\frac{\partial}{\partial t}\mathcal{E}_{x,y}+\left(\frac{\sigma}{\epsilon_r\,\epsilon_0}+\zeta\right)\mathcal{E}_{x,y} = \frac{1}{\epsilon_r\,\epsilon_0}\left(\nabla\times\vec{\mathcal{H}}\right)_{x,y}-\frac{1}{\epsilon_r\,\epsilon_0}\mathcal{J}_{x,y} \tag{46}$$

$$\frac{\partial}{\partial t}\mathcal{E}_{z}+\frac{\sigma}{\epsilon_r\,\epsilon_0}\mathcal{E}_{z} = \frac{1}{\epsilon_r\,\epsilon_0}\left(\nabla\times\vec{\mathcal{H}}\right)_{z}-\frac{1}{\epsilon_r\,\epsilon_0}\mathcal{J}_{z} \tag{47}$$

$$\frac{\partial}{\partial t}\mathcal{J}_{x,y}=\sigma\,\zeta\,\mathcal{E}_{x,y} \tag{48}$$

$$\frac{\partial}{\partial t}\mathcal{J}_{z}=-\zeta\left(\nabla\times\vec{\mathcal{H}}\right)_{z} \tag{49}$$

$$\frac{\partial}{\partial t}\mathcal{H}_{x,y}+\zeta\mathcal{H}_{x,y}=-\frac{1}{\mu_0}\left(\nabla\times\vec{\mathcal{E}}\right)_{x,y} \tag{50}$$

$$\frac{\partial}{\partial t}\mathcal{H}_{z}=-\frac{1}{\mu_0}\left(\nabla\times\vec{\mathcal{E}}\right)_{z}-\frac{1}{\mu_0}\mathcal{K}_z \tag{51}$$

$$\frac{\partial}{\partial t}\mathcal{K}_{z}=\zeta\left(\nabla\times\vec{\mathcal{E}}\right)_{z}. \tag{52}$$

Note that we have introduced a $1/\mu_0$ scaling factor into (51) and (52) to force their right-hand sides to have the same forms as the corresponding longitudinal electric field and polarization current equations. Discretization of the above differential equation set based on a standard Yee cell with both linear and exponential differencing has been performed and both differencing schemes produce essentially the same results. We implemented the numerical implementation approach discussed in [20], which uses the exponential differencing form, to produce the results presented below.

Numerical tests of a 2TDLM absorbing layer were performed in 1-D, 2-D, and 3-D FDTD simulators. In all cases, the simulations were performed with and without the 2TDLM layer, thus generating a known numerical solution for comparison. After obtaining the reference solution, the 2TDLM layer, consisting of ten cells and a perfect electric conductor (pec) backing, is then inserted into the problem space and the simulation is performed again. In the 1-D and 2-D simulations, both calculations were obtained simultaneously. In the 3-D simulations, this approach was not taken and the numerical reference solution was obtained independently to allow for larger simulation regions. The reflection caused by the introduction of the 2TDLM layer is then calculated at selected points in the grid by subtracting the reference solution from the solution containing the 2TDLM layer and then normalizing that difference by the maximum of the recorded reference field at that sample point.

The 1-D simulations considered the interaction of two periods of a 3.0-GHz plane wave modulated by a smooth envelope $\{1-[(t-T)/T]^4\}^2$ with the 2TDLM layer. The 2-D simulations considered the interaction of a normally incident 1-0-1 and a 2-2-2 pulsed, 3.0-GHz Gaussian beam with a waist of $0.1m$ with the 2TDLM layer. The m-n-p pulse profile consists of m cycles of rise time, n cycles of full amplitude oscillation and p cycles of fall time. Both of the 1-D and 2-D tests were run with $\lambda/20$ and $\lambda/50$ resolution. The 3-D simulation space, shown in Fig. 2, consisted of a lattice containing $100\Delta x\times100\Delta y\times100\Delta z$ square cells and ran for $500\Delta t$. A collimated, two-cycle 3.0-GHz Gaussian beam pulse with a waist of $0.1m$ and a 1-0-1 pulse profile was launched at normal incidence from a total field/scattered field plane ten cells in front of the air-dielectric interface. The 2TDLM model was introduced 30 cells into the lossy dielectric medium. Only the $\lambda/20$ resolution case was run in 3-D in order to allow us to implement, given the available memory, a very large electrical-sized simulation region.

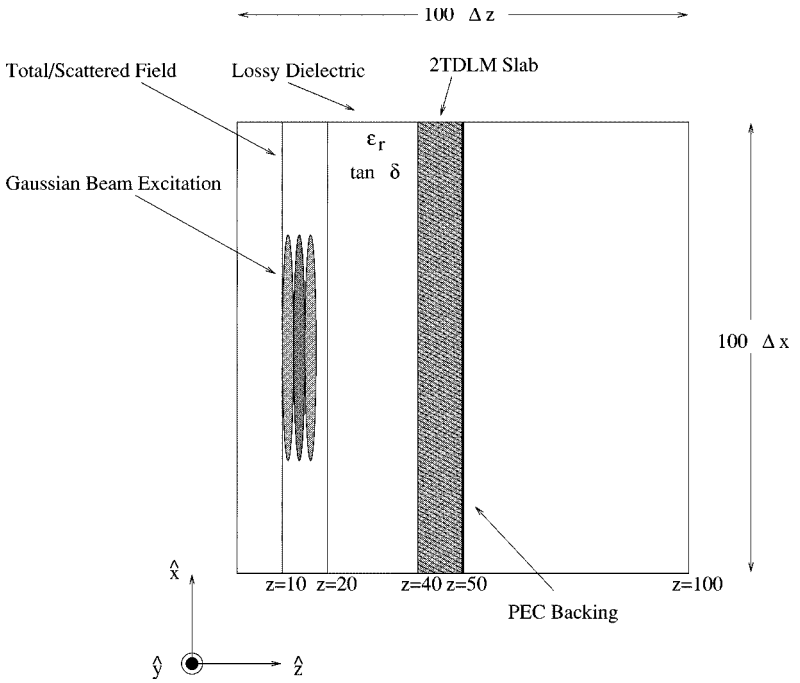

Fig. 2. 3-D problem space geometry.

Results were produced in 1-D, 2-D, and 3-D FDTD simulations at a resolution of $\lambda/20$. These analyses were completed for a dielectric (Duroid) with relative permeability $\epsilon_r = 2.2$ and two different loss tangents $\tan\,\delta = 0.1,\ 0.001$. The results of these calculations are shown in Fig. 3. Examination of the curves reveals that increasing the loss tangent by two orders of magnitude reduces the optimum value of $\overline{\zeta}_{\max}$ by two orders of magnitude. It is also noted that the 1-D, 2-D, and 3-D simulation cases are in rather good agreement despite the differences in the spatial dimensions and their different excitations. Since there is no analytic formula at present for determining the optimum value of $\overline{\zeta}_{\max}$, this agreement in 1-D, 2-D, and 3-D means that one can simply use the 1-D simulator to determine a good choice for $\overline{\zeta}_{\max}$ in the 2-D and 3-D situations. These 1-D simulations can be accomplished in a matter of minutes on a high performance workstation. Fig. 3 demonstrates that the 2TDLM slab is very effective as an absorber. Further, the selected value of $\overline{\zeta}_{\max}$ has a definite impact on the absorption qualities of the slab. In fact, it has a minimum value just as the PML ABC does [28]. The 1-D and 2-D simulations with the finer $\lambda/50$ resolution showed slightly better absorption levels despite the fact that the 2TDLM slab was electrically thinner, and the general behavior was the same as its parameters were varied.

It is common when doing numerical work to try and use as few cells as possible to implement a given model. This reduces the size of the model and makes simulations possible on computers of limited size. This is particularly critical for 3-D simulations. Thus, the effectiveness of the 2TDLM layer with varying thicknesses was next examined. Fig. 4 shows the reflection coefficient in 3-D for the $\tan\,\delta = 0.001$ case as a function of absorber thickness. The latter was determined in terms of the number of FDTD cells. The total thickness of the slab is $N\Delta z$.

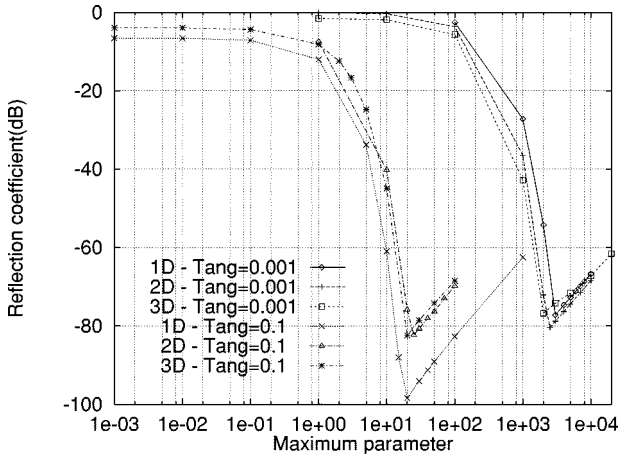

Fig. 3. Reflection coefficient versus $\overline{\zeta}_{\max}$ with $\lambda/20$.

Note the expected result that the reflection coefficient increases when using fewer cells in the absorbing layer. However, note that a high level of absorption is achieved even with relatively few number of cells.

V. Conclusions

The analytic solution for a general plane wave obliquely incident from a lossy electric and magnetic medium onto a biaxial anisotropic medium was presented and reformulated to take into account the polarization and magnetization fields responsible for the scattering. Selection criteria for the permittivity and permeability tensors, which provide reflectionless transmission through the interface, were found. A physical Maxwellian 2TDLM model was introduced to satisfy the matching conditions in addition to producing the desired loss

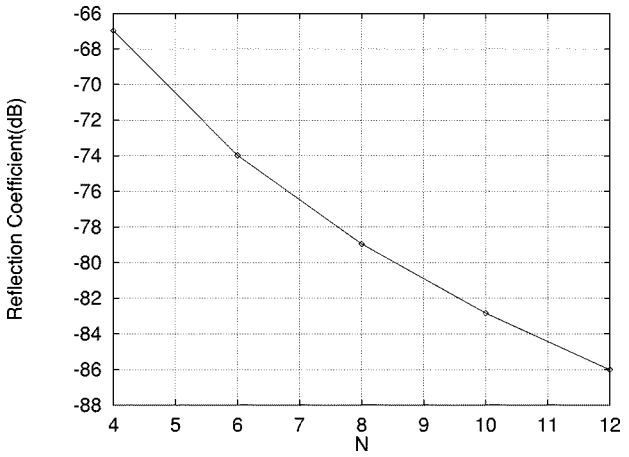

Fig. 4. Reflection coefficient versus N with $\lambda/20$ and $\tan\,\delta = 0.1$.

behavior. The final permittivity and permeability tensors for a 2TDLM absorbing layer were obtained from all of these conditions. A numerical implementation of this 2TDLM model was then derived for FDTD simulators. Numerical validation of the 2TDLM model was presented. It was demonstrated in 1-D, 2-D, and 3-D that a 2TDLM layer is a very effective matched absorber in the presence of lossy dielectric materials. Moreover, the similarity of the results in 1-D, 2-D, and 3-D provided justification to use the 1-D simulator to determine quickly the 2TDLM material constants for the 2-D and 3-D simulators.

Note that the lossy dielectric medium is naturally dispersive. By its very nature, the 2TDLM layer provides a means to terminate even more complex dispersive dielectric media. The procedure presented here can also be extended to lossy, dispersive magnetic media in a straightforward manner. It could be extended to lossy, dispersive electric and magnetic media as indicated in our analysis. However, the latter requires some extra considerations. There are several additional frequency terms that will appear because of the products and ratios of $\hat{\epsilon}_r$ and $\hat{\mu}_r$ and must be handled properly in the transition to the time domain. The same issue occurs in edge and corner regions if one extends the results here to achieve a full 3-D 2TDLM ABC since in those regions products of the permittivity and permeability tensors are required as discussed in [13] and [14]. Nonetheless, the results for the 2TDLM absorbing layer presented here clearly demonstrate that Maxwellian material models can be incorporated with standard FDTD solvers to define effective lossy layers which can be matched to any type of medium.

We note that while we have provided explicit results for FDTD simulators, the frequency domain version of the 2TDLM discussion can be applied immediately to FEM simulation regions. While the realization of absorbing layers matched to lossy dielectrics has many practical applications, this work, as noted in the introduction, also has applications toward the development of a complete absorbing boundary condition for numerical 3-D FDTD simulations of lossy dielectric regions. Such a 3-D 2TDLM ABC has been realized; its formulation and performance evaluation are reported in [20]. Moreover, applications of the 3-D 2TDLM ABC to microstrip line and micropatch antenna problems have been investigated; these results have been presented in [29].

REFERENCES

[1] J.-P. Berenger, "A perfectly matched layer for the absorption of electromagnetic waves," *J. Computat. Phys.*, vol. 114, pp. 185–200, Oct. 1994.
[2] D. S. Katz, E. T. Thiele, and A. Taflove, "Validation and extension to three dimensions of the Berenger PML absorbing boundary condition for FDTD meshes," *IEEE Microwave Guided Wave Lett.*, vol. 4, pp. 268–270, Aug. 1994.
[3] W. C. Chew and W. H. Weedon, "A 3-D perfectly matched medium from modified Maxwell's equations with stretched coordinates," *Microwave Opt. Technol. Lett.*, vol. 7, pp. 599–604, Sept. 1994.
[4] C. E. Reuter, R. M. Joseph, E. T. Thiele, D. S. Katz, and A. Taflove, "Ultrawideband absorbing boundary condition for termination of waveguiding structures in FDTD simulations," *IEEE Microwave Guided Wave Lett.*, vol. 4, pp. 246–344, Oct. 1994.
[5] C. M. Rappaport, "Perfectly matched absorbing boundary conditions based on anisotropic lossy mapping of space," *IEEE Microwave Guided Wave Lett.*, vol. 5, pp. 90–92, Mar. 1995.
[6] R. Mittra and Ü. Pekel, "A new look at the perfectly matched layer (PML) concept for the reflectionless absorption of electromagnetic waves," *IEEE Microwave Guided Wave Lett.*, vol. 5, pp. 84–86, Mar. 1995.
[7] Z. S. Sacks, D. M. Kingsland, R. Lee, and J.-F. Lee, "A perfectly matched anisotropic absorber for use as an absorbing boundary condition," *IEEE Trans. Antennas Propagat.*, vol. 43, pp. 1460–1463, Dec. 1995.
[8] A. Taflove, *Computational Electrodynamics: The Finite-Difference Time-Domain Method*. Boston, MA: Artech House, 1995.
[9] L. Zhao and A. C. Cangellaris, "GT-PML: Generalized theory of perfectly matched layers and its application to the reflectionless truncation of finite-difference time-domain grids," *IEEE Trans. Microwave Theory Tech.*, vol. 44, pp. 2555–2563, Dec. 1996.
[10] S. Gedney, "An anisotropic perfectly matched layer—Absorbing medium for the truncation of FDTD lattices," *IEEE Trans. Antennas Propagat.*, vol. 44, pp. 1630–1639, Dec. 1996.
[11] R. W. Ziolkowski, "The design of Maxwellian absorbers for numerical boundary conditions and for practical applications using engineered artificial materials," *IEEE Trans. Antennas Propagat.*, vol. 45, pp. 656–671, Apr. 1997.
[12] ——, "Time-derivative Lorentz materials and their utilization as electromagnetic absorbers," *Phys. Rev. E*, vol. 55, no. 6, pp. 7696–7703, June 1997.
[13] ——, "Time-derivative Lorentz material model-based absorbing boundary condition," *IEEE Trans. Antennas Propagat.*, vol. 45, pp. 1530–1535, Oct. 1997.
[14] ——, "Maxwellian material based absorbing boundary conditions," *Comp. Meth. Appl. Mech. Eng.*, vol. 169, no. 3/4, pp. 237–262, Feb. 1999.
[15] E. Turkel and A. Yefet, "Absorbing PML boundary layers for wave-like equations,", preprint, July 1997, to be published.
[16] S. Abarbanel and D. Gottlieb, "On the construction and analysis of absorbing layers in CEM," in *Proc. Appl. Computat. Electromagn. Soc.*, Monterey, CA, Mar. 1997, pp. 876–883.
[17] R. W. Ziolkowski and F. Auzanneau, "Passive artificial molecule realizations of dielectric materials," *J. Appl. Phys.*, vol. 82, no. 7, pp. 3195–3198, Oct. 1997.
[18] ——, "Artificial molecule realization of a magnetic wall," *J. Appl. Phys.*, vol. 82, no. 7, pp. 3192–3194, Oct. 1997.
[19] F. Auzanneau and R. W. Ziolkowski, "Theoretical study of synthetic bianisotropic smart materials," *J. Electromagn. Waves Applicat.*, vol. 12, no. 3, pp. 353–370, Mar. 1999.
[20] D. C. Wittwer and R. W. Ziolkowski, "Maxwellian material based absorbing boundary conditions for lossy media in 3-D," IEEE Trans. Antennas Propagat., Aug. 1998, submitted for publication.
[21] S. D. Gedney, "An anisotropic PML absorbing media for FDTD simulation of fields in lossy dispersive media," *Electromagn.*, vol. 16, pp. 399–415, July/Aug. 1996.
[22] A. Taflove, *Advances in Computational Electrodynamics: The Finite-Difference Time-Domain Method*. Boston, MA: Artech House, 1998.
[23] Y. C. Lau, M. S. Leong, and P. S. Kooi, "Extension of Berenger's PML boundary condition in matching lossy medium and evanescent waves," *Electron. Lett.*, vol. 32, no. 11, pp. 974–976, 1996.

[24] J. Fang and Z. Wu, "Generalized perfect matched layer for the absorption of propagating and evanescent waves in lossless and lossy media," *IEEE Trans. Microwave Theory Tech.*, vol. 14, pp. 2216–2222, Dec. 1996.
[25] Q. H. Liu, "An FDTD algorithm with perfectly matched layers for conductive media," *Microwave Opt. Technol. Lett.*, vol. 14, pp. 134–137, Feb. 1997.
[26] C. M. Rappaport and S. C. Winton, "Modeling dispersive soil for FDTD computation by fitting conductivity parameters," in *Proc. Appl. Computat. Electromagn. Soc.*, Monterey, CA, Mar. 1997, pp. 112–117.
[27] J. Kong, *Electromagnetic Waves*. New York: Wiley, 1986, pp. 110–111.
[28] D. C. Wittwer and R. W. Ziolkowski, "How to design the imperfect Berenger PML," *Electromagn.*, vol. 16, pp. 465–485, July/Aug. 1996.
[29] ——, "The effect of dielectric loss in FDTD simulations of microstrip structures," IEEE Trans. Microwave Theory Tech., submitted for publication.

David C. Wittwer (S'93–M'95) received the B.S., M.S., and Ph.D. degrees in electrical engineering from the Department of Electrical and Computer Engineering at the University of Arizona, Tucson, AZ, in 1993, 1995, and 1998, respectively.

He was a member of the technical staff at Hughes Missile Systems Company, Tucson, AZ, from 1995 to 1999. While at Hughes, he received the Howard Hughes Doctoral Fellowship. His work at Hughes involved the analysis, design, and measurement of microstrip and slot arrays for missile seeker and telemetry antennas. In 1999 he joined the assembly and test development group at Intel Corporation, Chandler, AZ, where he is a Senior Packaging Engineer. His focus area is in electromagnetic compatibility and interference compliance of computer microprocessors. His research interests include the development and implementation of time-domain electromagnetic solvers.

Dr. Wittwer is a member of IEEE Antennas and Propagation, Microwave Theory and Techniques, and Electromagnetic Compatibility societies.

Richard W. Ziolkowski (M'87–SM'91–F'94) received the Sc.B. degree in physics magna cum laude (with honors) from Brown University, Providence, RI, in 1974, and the M.S. and Ph.D. degrees in physics from the University of Illinois at Urbana-Champaign, in 1975 and 1980, respectively.

From 1981 to 1990, he was a member of the Engineering Research Division at the Lawrence Livermore National Laboratory and served as the Leader of the Computational Electronics and Electromagnetics Thrust Area for the Engineering Directorate from 1984 to 1990. He joined the Department of Electrical and Computer Engineering at the University of Arizona as an Associate Professor in 1990 and was promoted to Full Professor in 1996. He was a coguest editor of the 1998 feature issue of the *Journal of the Optical Society of America A* on mathematics and modeling in modern optics. His research interests include the application of new mathematical and numerical methods to linear and nonlinear problems dealing with the interaction of acoustic and electromagnetic waves with realistic materials and structures.

Dr. Ziolkowski is a member of Tau Beta Pi, Sigma Xi, Phi Kappa Phi, the American Physical Society, the Optical Society of America, the Acoustical Society of America, and Commissions B (Fields and Waves) and D (Electronics and Photonics) of URSI (International Union of Radio Science). He was an Associate Editor for the IEEE TRANSACTIONS ON ANTENNAS AND PROPAGATION from 1993 to 1998. He served as the Vice Chairman of the 1989 IEEE/AP-S and URSI Symposium in San Jose, CA, and as the Technical Program Chairperson for the 1998 IEEE Conference on Electromagnetic Field Computation in Tucson, AZ. For the U.S. URSI Commission B, he served as Secretary from 1993 to 1996 and as Chairperson of the Technical Activities Committee from 1997 to 1999. He will serve as a Member-at-Large of the U.S. National Committee (USNC) of URSI in 2000. He was a coorganizer of the Photonics Nanostructures Special Symposia at the 1998 and 1999 OSA Integrated Photonics Research Topical Meetings. He was awarded the Tau Beta Pi Professor of the Year Award in 1993 and the IEEE and Eta Kappa Nu Outstanding Teaching Award in 1993 and 1998, respectively.